Gas Storage in Structure H Hydrates

A. A. Khokhar[1], J. S. Gudmundsson[1], and E. D. Sloan [2,3]

[1]Norwegian University of Science and Technology, Department of Petroleum Engineering and applied Geophysics, N-7034 Trondheim, Norway.

[2] Center for Hydrate Research, Colorado School of Mines, Golden, CO 80401, USA

[3] Corresponding author

Keywords: enthalpy, gas storage, hydrate, promoter, solid-fluid equilibria, structure H

ABSTRACT

Four aspects of the storage of methane in structure H hydrate were investigated: (1) four phase (L_W-H-V-L_{HC}) pressure-temperature equilibrium data are reported for 1,3-dimethylcyclohexane, a new structure H hydrate former, (2) in comparison with other hydrate structures it was shown that methane storage in sH hydrate is an attractive alternative if the large cage of sH is occupied with a large guest while the small cages are occupied by methane, (3) polyvinylpyrrolidone (PVP) was found to promote the amount of hydrate formation, and (4) heats of dissociation (ΔH^{diss}) below 0 ^{o}C were estimated to have ±20% variation for all three hydrate structures (sI, sII, and sH).

1. INTRODUCTION

Natural gas clathrate hydrates are cage-like assemblages of water molecules around gas molecules, often referred as hosts and guests. Hydrates are ice-like except that they can form at high pressure and temperatures above the ice point as a function of the gas composition [1,2]. There are three known structures in which water molecules arrange themselves around guest molecules, depending principally upon the molecular size of the guest molecules (Figure 1).

Based on structure I (sI) and structure II (sII) hydrate studies, it was thought that n-butane was the largest natural gas molecule which could form hydrate. The discovery of structure H (sH) hydrate in 1987 by Ripmeester et al.[3] and the subsequent discovery of sH hydrate in nature by Sassen et al.[4] suggested that a new range of petroleum components can form sH hydrates in subsea pipelines. This paper consider the implications of gas storage in sH hydrate.

This work was undertaken to investigate four practical questions regarding physical properties of sH hydrates:

1. Is it possible that other large molecules can form structure H?
2. How practical is it to consider storage of methane in sH if the large cavities are filled with a large molecule?
3. Is it possible to chemically assist sH hydrate formation, so that more moles of gas and water convert to hydrate?
4. What is the heat of dissociation ΔH^{diss} of sH below the ice point, and how does it compare to other hydrate structures?

Each of these questions is introduced in the remainder of this section.

1.1 Size of Large Structure H Guests

Previous data by Mehta [5] measured four phase equilibrium data for 15 liquid hydrocarbons with methane as the help gas. Molecules as large as 9.25Å (2,2-dimethylpentane) formed in the large $5^{12}6^{8}$ cage of sH hydrate, although Thomas and Behar [6] measured two data points for ethylcyclohexane, a very large molecule (9.77Å). While Ripmeester et al. [7] indicated that both size and shape were significant parameters we wished to determine if other large molecules were sH formers.

1.2 Storage of Natural Gas in Hydrates

Storage of natural gas in hydrates have been investigated since their discovery [8] because hydrates store large quantities (e.g. 180 SM^3 per M^3 of hydrate) of gas [1,9]. Two storage methods has been suggested: either keeping hydrate under low temperature [10,11] or under high pressure [12,13]. Recently, Gudmundsson et al.[14] showed that sII hydrate can be stored at -15 ^{o}C under atmospheric pressure for 15 days, retaining almost all the gas. Later, they [15] also published a feasibility study showing a substantial cost saving (24%) for the transport of natural gas in hydrated form compared to liquefied natural gas (LNG) form the northern North Sea to the Central Europe. Saito et al. [16] measured methane stored in small cages of sII hydrate using tetrahydrofuran, an aqueous-miscible compound which occupies the large sII cages ($5^{12}6^{4}$).

The best option for methane storage is sI hydrate because methane will occupy both small and large cavities (1), however high formation pressures are required. To reduce high methane formation pressures, we considered filling the large cage in sI ($5^{12}6^{2}$) and that in sII ($5^{12}6^{4}$) with a large miscible molecule like ethylene oxide and tetrahydrofuran

respectively, so that methane would occupy principally the small 5^{12} cages. Similarly, for sH hydrate the largest cage ($5^{12}6^{8}$) was stabilized with a large molecule and the methane occupied the smaller 5^{12} and $4^{3}5^{6}6^{3}$ cages.

Table 1 shows a calculated comparison of methane storage in all three hydrate structures with total occupation of small cages by methane and a second large molecule occupying all large cages. This would be the maximum storage potential of methane in three hydrate structures with methane occupying only small cages. The second column of Table 1 show a comparison of the maximum gas volumes (STP) contained in a unit volume of hydrate. The amount of methane stored in the small cages of sH is significantly higher than either sI or sII, but only one-third of the LNG [17] capacity. An energy density of methane is shown in the third column of Table 1 for each hydrate structure and LNG. The energy values are also compared with liquefied natural gas (LNG) at -160 ^{o}C.

The above calculations indicate that sH hydrate can store the largest amount of methane principally because the ratio of small to large cages is 5:1, compared to 2:1 for sII and 1:3 for sI, with roughly comparable unit structure sizes of 1323 Å^{3}, 5177 Å^{3}, and 1728 Å^{3} for sH, sII and sI respectively. We decided to investigate the storage option of methane gas in sH hydrate with the largest cage stabilized by 2,2-dimethylbutane. It should be noted that sH hydrate required at least two components i.e. the large molecule like 2,2-dimethylbutane in the $5^{12}6^{8}$ cage and a help-gas like methane in 5^{12} and $4^{3}5^{6}6^{3}$ cages.

1.3. Promoting the Conversion of Water to Hydrate

Hydrate tend to form at the vapor-water interface, due to the mutual immiscibility of each phase and the high contents of gas and liquid in hydrate, formation at the interface may block further conversion of water to hydrate so that liquid water is trapped (or occluded) within or under the solid hydrate. Many workers [16,18] have tried various options to reduce occluded water i.e. high agitation, increasing surface area, and using a miscible hydrate former. Here we wished to investigate the data from the Center for Hydrate Research [19] which indicated that polyvinylpyrrolidone (PVP), a kinetic inhibitor, might act as a hydrate promoter to prevent occlusion of water when used in very low concentrations at high pressures.

1.4 Determining the Heat of Hydrate Dissociation

After transportation, hydrates are dissociated to recover gas under atmospheric conditions. Hydrate melting can occur both above and below 0 ^{o}C [14], so that the heat of dissociation (ΔH^{diss}) of hydrate below 0 ^{o}C will be an import process design parameter. However, while there are ΔH^{diss} values reported for sI, sII, and sH above 0 ^{o}C [20,5] there are neither experimental nor estimated ΔH^{diss} data below 0 ^{o}C for sH hydrate. There are only three experimental ΔH^{diss} values reported below 0 ^{o}C for natural gas (sI and sII) components [21]. These ΔH^{diss} were calculated for a wide range of temperatures below 0 ^{o}C using heat capacity data. The fourth objective of this work was to determine ΔH^{diss} for sH below 0 ^{o}C and to compare it with values for sI, and sII.

2. APPARATUSES AND PROCEDURE

2.1. Measurements above the Ice Point

The apparatus is shown in Figure 2 for measuring four phase (L_W-H-V-L_{HC}) equilibrium pressure-temperature data for chemicals which form sH hydrate. The apparatus consisted of a rocked Jerguson sight glass, immersed in a constant temperature bath. The temperature of the cell was monitored with a platinum resistance probe accurate to ±1%, and the pressure was measured using a Heise pressure gauge accurate to ±20.7 kPa.

The cell was charged with 75.0 cc of distilled, deionized water and 28.0 cc (100% stoichiometric excess) of 1,3-dimethylcyclohexane. There were 25 stainless steel balls (0.79 cm diameter) in the cell for agitation of fluids during rocking. The cell was pressurized with methane gas above the sI hydrate equilibrium pressure. The rocking of the cell started when temperature and pressure were stabilized.

In this way, sI was initially formed in order to create hydrogen bonds. Later, the cell pressure was dropped below the sI formation pressure to dissociate sI hydrate. When all sI hydrate dissociated, the pressure in the cell was raised to a value below the sI hydrate equilibrium condition. After a significant amount of sH hydrate formed, the pressure was decreased to dissociate sH hydrate. By this trial and error procedure the equilibrium pressure was determined to ±17.2 kPa. The experimental procedure is identical to that reported by Mehta et al. [5] as shown schematically in Figure 4.

Methane gas storage experiments in sH were also performed in the Jerguson cell (Figure 2) by charging the cell with 50.0 cc distilled, deionized water and 8.0 cc (10% stoichiometric excess) of 2,2-dimethylbutane. After evacuation, the cell was pressurized

with methane gas below the equilibrium of sI hydrate from a 1055.1 cc gas cylinder. Upon temperature stabilization in the cell, rocking of the cell was started and sH hydrate appeared in a few minutes. Gas hydrate formation was assumed to be completed when there was no further pressure drop observed in the cell. The pressure and temperature of the methane supply cylinder and sight glass cell were monitored for gas consumption as well as an indication of hydrate formation.

Methane storage experiments were also conducted using a small weight percent (wt%) polyvinylpyrrolidone (PVP) as hydrate promoters. Three types of experiments were conducted for monitoring methane storage in sH:

I. at constant volume, the pressure decreased as hydrate formed,
II. after hydrate formation, when the cell temperature decreased to the bath temperature, the pressure was again increased, and
III. the cell pressure was maintained constant within ±138 kPa without consideration to temperature increase due to hydrate formation in the cell.

2.2. Measurements Below the Ice Point

Hydrate equilibrium pressure measurements below 0 ^{o}C were conducted on the apparatus shown in Figure 3 for binaries of sI, sII, and sH hydrates. The spherical steel reactor (5.08 cm I.D. rated for 10.1 MPa) was submerged in propylene glycol in a 8.0 liter Neslab stirred bath. The reactor cell contained 150 stainless steel balls (0.31 cm diameter) and was agitated via a Thermolyne orbital shaker with 0.4 cm amplitude.

The temperature was maintained via a 600 Watt immersion heater and the Neslab controller to within ±0.3 K. Temperature were obtained with an Omega platinum resistance thermometer (±0.1 K accuracy) and pressure was monitored via 13.43 MPa and

2.01 MPa Heise gauges accurate to 1% of full scale. A Barocell differential electronic manometer (0.267 MPa full scale, 0.133 Pa resolution) was used at low pressures. Water and liquid hydrocarbon were vacuum distilled into the reactor.

The cell was charged with methane or a binary mixture. For sH measurements, sI hydrate was initially formed, with subsequent dissociation by decreasing the pressure to conditions below the sI equilibrium. A pressure search procedure identical to that of Makogon et al.[30] below 0 ^{o}C was adopted, as shown schematically in Figure 4. The final equilibrium pressure was determined to ±17.2 kPa.

3. EXPERIMENTAL RESULTS AND DISCUSSION

3.1 New Structure H Former

Phase equilibrium conditions were determined for a new sH former, 1,3-dimethylcyclohexane, discovered during this work with methane as help gas. The ten phase (L_W-H-V-L_{HC}) equilibrium pressure and temperature data are plotted in Figure 5 and listed in Table 2 along with the large guest molecular structure. The molecular size of 1,3-dimethylcyclohexane was determined with Hyper-Chem® as 9.293Å. Due to large size of 1,3-dimethylcyclohexane, the kinetics of hydrate formation were slow, requiring about four weeks to obtain the data listed (Table 2). The diameter of 1,3-dimethylcyclohexane relative to the $5^{12}6^{8}$ cavity is 0.814. Based on similar data for sI and sII guest:cavity ratios [1], it appears that there are other larger molecules which can form sH hydrate.

3.2 Methane Storage In sH Hydrate

Summary results for methane consumption during the three types of experiments (described at the end of Section 2.1) are given in Table 3. In every case PVP encourage

more water and gas (n_g/n_w) to convert to hydrate than without PVP at comparable concentration. An increased gas storage during type II experiments can be explained by high driving force (pressure) for hydrate formation. Comparing experiments type II and III indicate that continuous heat removal can promote hydrate production.

3.3 Increased sH Hydrate Formation With Promoter (PVP)

In the second phase, experiments in the preceding section were modified to add 0.1wt% (weight percent) PVP in 50.0 cc of distilled deionized water and 8.0 cc of 2,2-dimethylbutane. Our experiments used a maximum hydrate formation pressure of 3.3 MPa or less, so the storage technique could be feasible at common process conditions.

A hypothesis suggests the increased water conversion to hydrate in the presence of PVP. Figure 6a is a hydrate particle grown without hydrate promoter. Once critical nuclei are formed, hydrate grows very rapidly and occlude significant water. PVP may prevent occluded water for two reasons. First if hydrate formed slowly they prevent occluded water. Secondly the hydrate morphology is changed from block, ice-like hydrate to a dendritic structure, so that occlusion is more difficult (Figure 6b). T. Y. Makogon [22] showed that PVP inhibition is caused by a long polymer backbone adsorbing with its pendent groups in partially-completed cavities on the hydrate surface. This adsorption causes a change in crystal morphology and slows the growth, thus inhibiting water occlusion.

3.4 Hydrate ΔH^{diss} Below 0^0C

Because ΔH^{diss} values estimated above 0 ^oC using Clausius-Clapeyron equation were within an acceptable accuracy [20] and since measurements via calorimeters are

painstaking [23], we used univariant phase equilibrium data below 0 ^{o}C to calculate ΔH^{diss} using the Clausius-Clapeyron equation, i.e.

$$\frac{d\ln P}{d\left(1/T\right)} = -\frac{\Delta H^{diss}}{zR}$$

where P and T are equilibrium absolute pressure and temperature respectively, z is the gas compressibility and R is the universal gas constant. The above equation can be used to calculate ΔH^{diss} if hydrate equilibrium (P-T) data are known for a univariant system (e.g. three components and four phases, or two components and three phases).

Figure 7 shows a plot of *ln P* vs. *1/T* below 0 ^{o}C for pure gases and for a methane-ethane binary which forms sI hydrate. Slopes of the lines in Figure 7 vary by ±14.5% for different sI formers. A similar plot is shown in Figure 8 for pure gases as well as binary mixtures that form sII hydrate. Slope trends similar to those for sI and sII hydrates were also observed for sH hydrate (Figure 9) below 0 ^{o}C. Here slopes (*lnP* vs. *1*/*T*) varied for sH by ±17% using different help gases. Similar trends in sH hydrate above 0 ^{o}C were observed by Mehta [5].

Table 4 summarizes the results of calculated ΔH^{diss} using slopes of equilibrium data (*lnP* vs. *1*/*T*) in the Clausius-Clapeyron equation below 0 ^{o}C. ΔH^{diss} for all three hydrate structures vary within ±19%. This similarity may be due to the fact that hydrate are 85 mole percent water with only 15 mole percent gas, so the hydration number is approximately equal.

4. CONCLUSIONS

1. Ten phase equilibrium data are reported for a new chemical (1,3-dimethylcyclohexane) which forms sH hydrate.
2. Methane storage appears promising in sH hydrate relative to storage in sI or sII when methane occupies only the small cavities. Storage capability in sH was verified using pure water.
3. Formation kinetics of sH hydrate were enhanced with the addition of PVP as more methane was consumed during hydrate formation in the presence of PVP than in the case of pure water.
4. Heats of dissociation below 0 ^{o}C for sI, sII, and sH hydrates were estimated using univariant pressure-temperature equilibrium data and the Clausius-Clapeyron equation. The results showed only 19% variation in the ΔH^{diss} between three hydrate structures.

5. ACKNOWLEDGMENT

The financial assistance for A. A. Khokhar from Aker Engineering (Oslo, Norway) through the NGH project at NTNU is greatly appreciated.

6. REFERENCES

[1] E. D. Sloan, Clathrate Hydrate of Natural Gases, Marcel Dekker, New York, 1990.

[2] E. D. Sloan, 213th ACS National Meeting, San Francisco, CA, Vol. 42, No. 2, April 13-17, 1997, pp. 449-456

[3] J. A. Ripmeester and C. I. Ratcliffe, J. Phys. Chem. 1990, 94, pp. 8773-8776.

[4] R. Sassen and I. R. MacDonald, Org. Geochem., Vol. 22, No. 6, pp. 1029-1032.

[5] A. P. Mehta, A thermodynamic investigation of structure H clathrate hydrate, Ph.D. thesis, 1996, Colorado School of Mines, Golden, CO.

[6] M. Thomas, E. Behar, Structure H hydrate equilibria of methane and intermediate hydrocarbon molecules, 73rd GPA convention, New Orleans, March 7- 9, 1994.

[7] J. A. Ripmeester, C. I. Ratcliffe and G. E. McLaurin., The role of heavier hydrocarbons in hydrate formation, AIChE meeting, Houston, 1991.

[8] E. G. Hammerschmidt, Oil Gas J. 1939, pp. 66.

[9] Y. F. Makogon, Hydrates of Natural Gas, PennWell Books, Tulsa, OK, 1981.

[10] B. Miller and E. R. Strong, A.G.A. Proceedings, 27, 50, 1945.

[11] M. E. Benesh, U.S. Patent No. 2,270,016 (1942).

[12] D. Berner, Proc. of 2nd Internl. Offshore and Polar Eng. Conf., San Francisco, CA, 14-19 June, 1992, pp. 636-643.

[13] N. V. Chersky, U.S. Patent No. 3,888,434 (1975).

[14] J.-S. Gudmundsson, M. Parlaktuna, and A. A. Khokhar, SPE Prod. & Facil., Feb. 1994.

[15] A. Børrehaug and J. S. Gudmundsson, Proceedings Eurogas, 3-5 June, 1996.

[16] Y. Saito et al., in Proc. 2nd Intnl. Conf. on Natural Gas Hydrates, J. P. Monfort, (Ed.), Toulouse, 2-6 June, 1996, pp. 459-465.

[17] A. J. Kidnay, Liquefied Natural Gas, Min. Indust. Bulletin, Vol. 15, No.2, 1972.

[18] R. Rogers, G. Yevi, and M. Swalm, in Proc. 2nd Intnl. Conf. on Natural Gas Hydrates, J. P. Monfort, (Ed.), Toulouse, 2-6 June, 1996, pp. 423-429.

[19] J. P. Lederhos et al., Chem. Eng. Sci., Vol. 51, No. 8, 1996, pp. 1221-1229.

[20] E. D. Sloan and F. Fleyfel, Fluid Phase Equilibria, 76, 1992, pp. 123-140.

[21] Y. P. Handa, J. Chem. Thermodynamics, 1986, 18: pp. 915-921.

[22] T. Makogon, Experimental and computer study of the effect of kinetic inhibition on clathrate hydrates, Ph.D. thesis, 1996, Colorado School of Mines, Golden, CO.

[23] Y. P. Handa, Chem. Thermodynamics 1985, 18, 891.

[24] W. M. Deaton, E. M. Frost Jr., Gas hydrates and their relation to the operation of natural gas pipelines, U.S. Bureau of Mines Monograph 8, 1946, pp. 101.

[25] O. L. Roberts, E. R. Brownscombe, L. S. Howe, Oil & Gas J., 39, (30), 37 (1940).

[26] S. D. Larson, Phase studies of the two-component carbon dioxide-water system, involving the carbon dioxide hydrate, Univ. Illinois, 1955.

[27] F. T. Selleck, L. T. Carmichael, B. H. Sage, Ind. Eng. Chem., 44, 2219 (1952).

[28] G. D. Holder, S. P. Godbole, AIChE Journal, 28, 930, 1982.

[29] G. R. Schneider, J. Farrar, U.S. Dept. of Interior, Rsch. Dev. Rpt. No. 292, pp. 37, January 1968.

[30] T. Y. Makogon, A. P. Mehta and E. D. Sloan, J. Chem. Eng. Data, Vol. 41, No. 2 1996, pp. 315-318.

[31] J. L. de Roo, C. J. Lichtenthaler, G. A. M. Diepen, AIChE J., 29, 651 (1983).

[32] V. T. John, G. D. Holder, J. Phys. Chem., 86, 455, (1982).

List of Tables

Table 1
Calculated maximum methane storage potential in the small cavities of all three hydrate structures by stabilizing the large cavity with large molecule.

Table 2
Hydrate equilibrium data of 1,3-Dimethylcyclohexane, a new sH hydrate former.

Table 3
Methane gas storage in sH with pure water and with 0.1wt% PVP as hydrate promoter.

Table 4
Heat of dissociation (ΔH^{diss}) estimated with Clausius-Clapeyron equation for three hydrates structures below 0 ^{o}C.

List of Figures Captions

Figure 1: Three type of hydrate structures and their cage arrangement.

Figure 2: Schematic of apparatus for equilibrium measurements (adopted from Mehta [5]) and gas storage experiments.

Figure 3: Apparatus schematic used in hydrate equilibrium measurement below 0 ^{o}C (adopted from Makogon [30]).

Figure 4: Search procedure for hydrate equilibrium pressure (adopted from [5,30]) at constant temperature.

Figure 5: sH hydrate equilibrium for 1,3-Dimethylcyclohexane, a new sH former.

Figure 6: Microscopic cartoon of a block hydrate growth (a) without PVP and dendritic growth (b) with PVP.

Figure 7: *ln* P versus 1/T below 0 ^{o}C for single component and a binary mixture forming sI hydrate.

Figure 8: *ln* P versus 1/T below 0 ^{o}C for pure components and binaries forming sII hydrate.

Figure 9: Equilibrium *ln* P versus 1/T for sH hydrate below 0 ^{o}C using methane and xenon as help gas.

Table 1
Calculated maximum methane storage potential in the small cavities of all three hydrate structures by stabilizing the large cavity with large molecule.

Small Cages for Methane	**Vol. of Methane (m^3)**	**Energy Density $kcal/m^3$**
sI in 5^{12}	56.02	$5.32 \cdot 10^5$
sII in 5^{12}	154.08	$1.46 \cdot 10^6$
sH in 5^{12} & $4^3 5^6 6^3$	200.93	$1.90 \cdot 10^6$
LNG @ -160 ^oC	600.0	$6.00 \cdot 10^6$

Table 2
Hydrate equilibrium data of 1,3-Dimethylcyclohexane, a new sH hydrate former.

Temperature (K)	Pressure (MPa)
275.99	3.07657
276.93	3.31440
277.50	3.60300
278.43	4.09443
278.99	4.25481
279.47	4.39481
280.59	5.11042
281.43	5.67800
281.99	6.01415
282.47	6.35959

Table 3
Methane gas storage in sH with pure water and with 0.1wt% PVP as hydrate promoter.

Experimental Conditions
Volume of Water = 50.0 cc
Volume of 2,2-Dimethylbutane = 8.0 cc
Temperature of Cell = 275.5 K
Pressure of Cell <= 3200 kPa (lower than methane equilibrium pressure)

Water Conversion to Hydrate

Expt. Type (See Text)	**No PVP** H_2O to Hydrate	**With PVP** H_2O to Hydrate
I	20.83%	22.75%
II	26.08%	40.99%
III	15.62%	17.55%

Gas:Water mole[1] ratio in Hydrates

Expt. Type (See Text)	**No PVP** $\mathbf{n_g/n_w}$ (mol/mol)	**With PVP** $\mathbf{n_g/n_w}$ (mol/mol)
I	3.17%	3.47%
II	3.97%	6.24%
III	2.38%	2.67%

[1] The maximum gas:water mole ratio in hydrates is 15%.

Table 4

Heat of dissociation (ΔH^{diss}) estimated with Clausius-Clapeyron equation for three hydrates structures below 0 ^{o}C.

Structure Type	Guest Composition	Slope (1/K)	ΔH^{diss} (kJ/gas-mole)
sI	Methane	-2437.44	-19.13
	Ethane	-3043.83	-24.37
	Methane + Ethane	-3193.20	-25.67
	Carbon Dioxide	-3011.72	-23.89
	Hydrogen Sulfide	-2916.28	-24.03
	Average Value	**-2852.32**	**-23.42**
sII	Propane	-3583.62	-28.96
	i-Butane	-3544.45	-28.64
	Methane + Propane	-3361.48	-27.53
	Methane + n-Butane	-3533.02	-28.17
	Average Value	**-3505.64**	**-28.33**
sH	Methane + Methylcyclohexane	-2847.49	-23.06
	Methane + Neohexane	-2872.07	-23.33
	Xenon + Neohexane	-3450.44	-28.43
	Average Value	**-3056.67**	**-24.94**

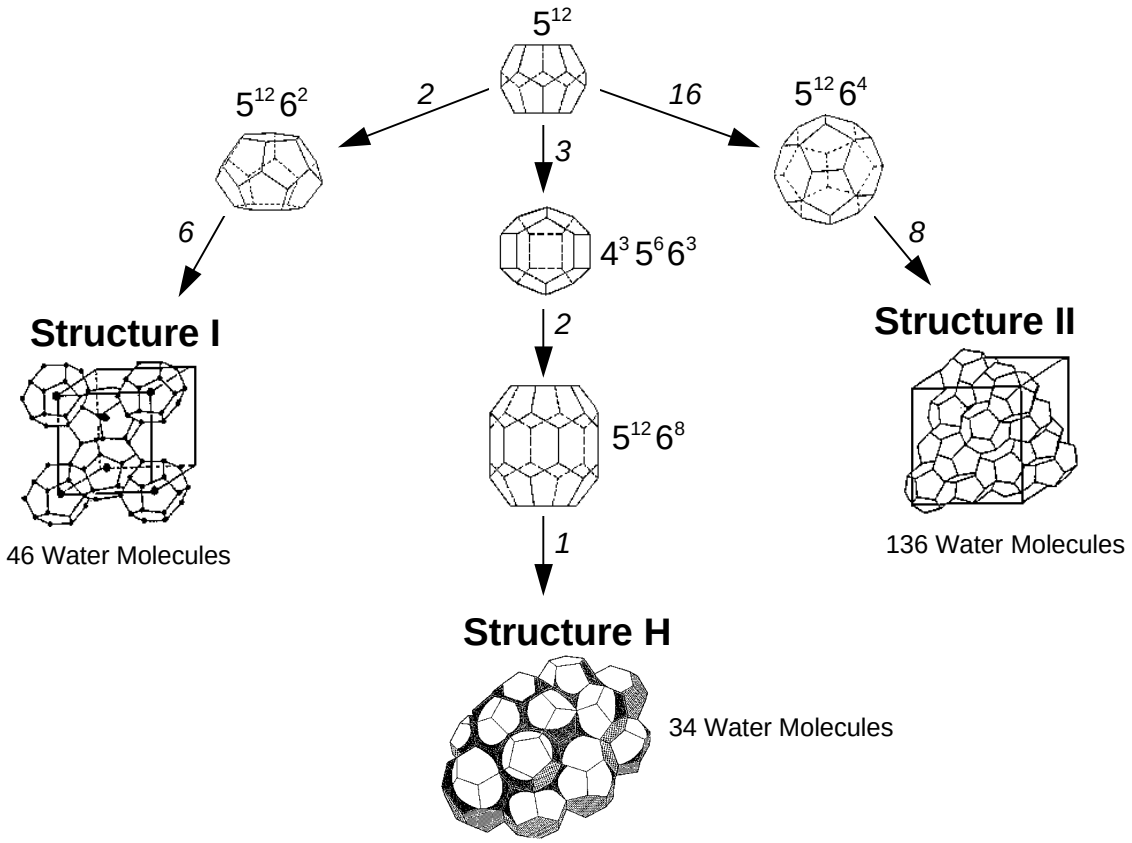

Figure 1: (Khokhar et al.)

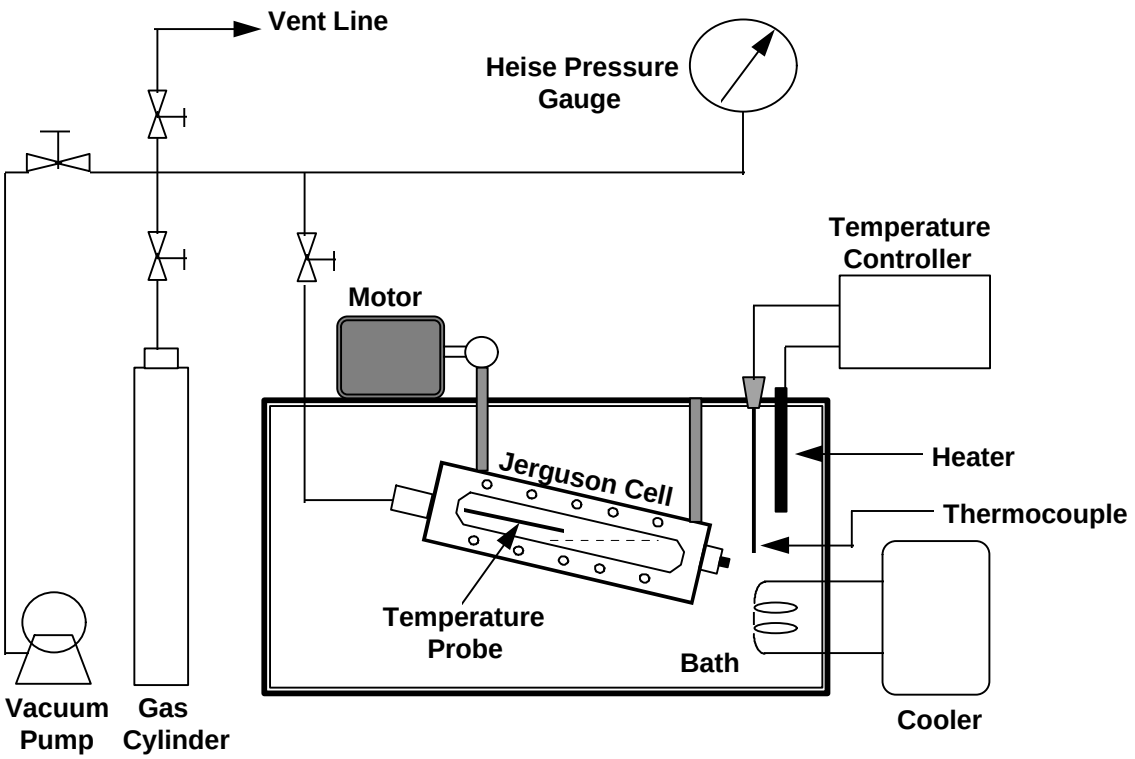

Figure 2: (Khokhar et al.)

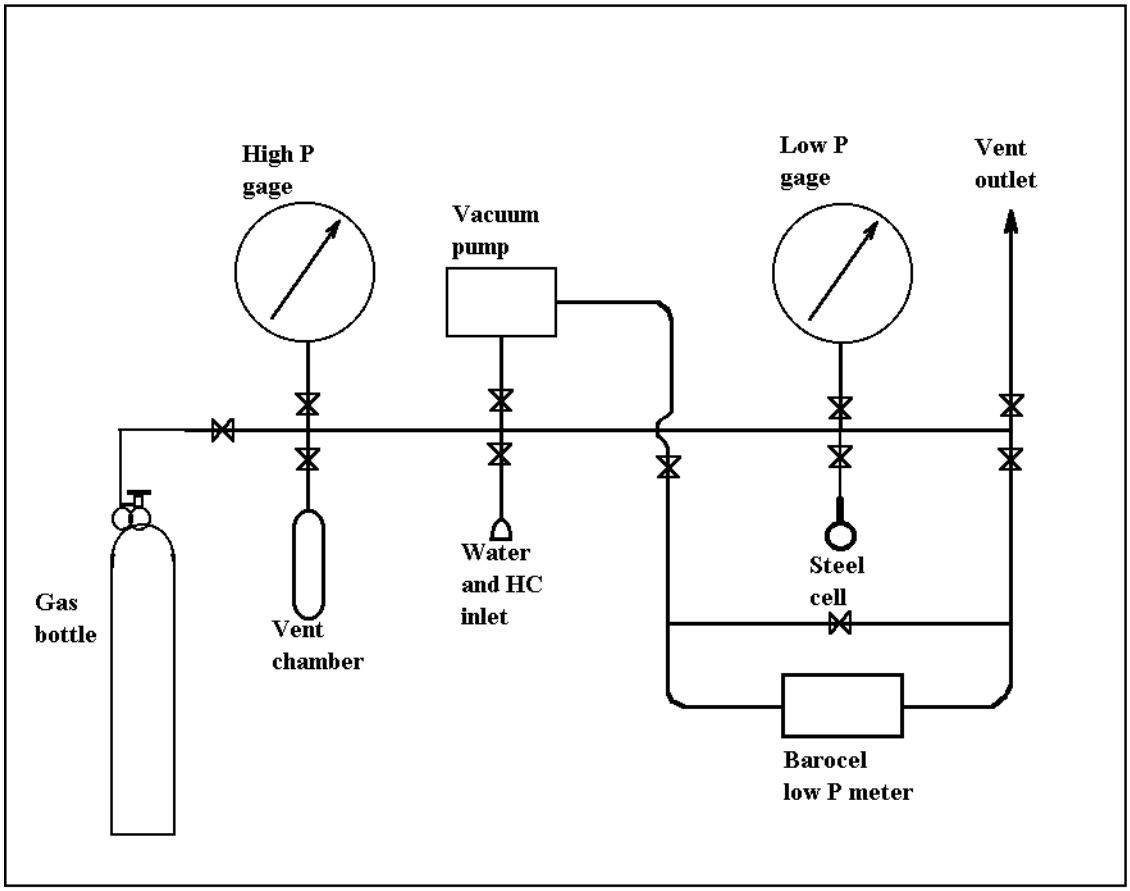

Figure 3: (Khokhar et al.)

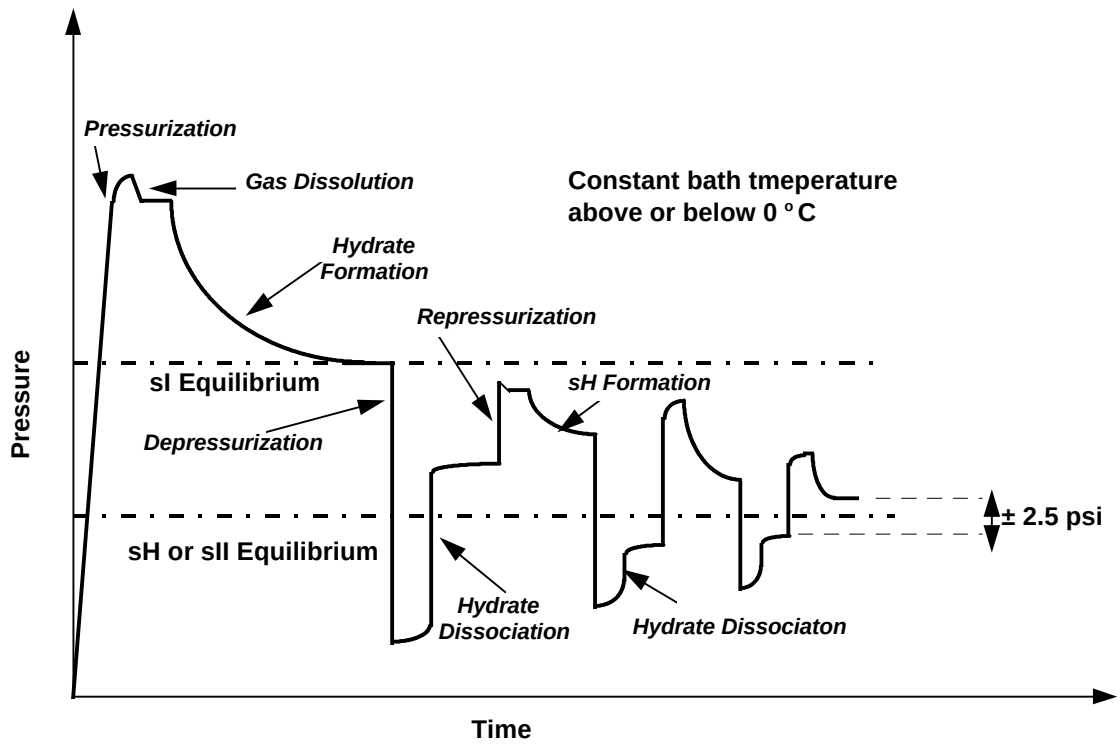

Figure 4: (Khokhar et al.)

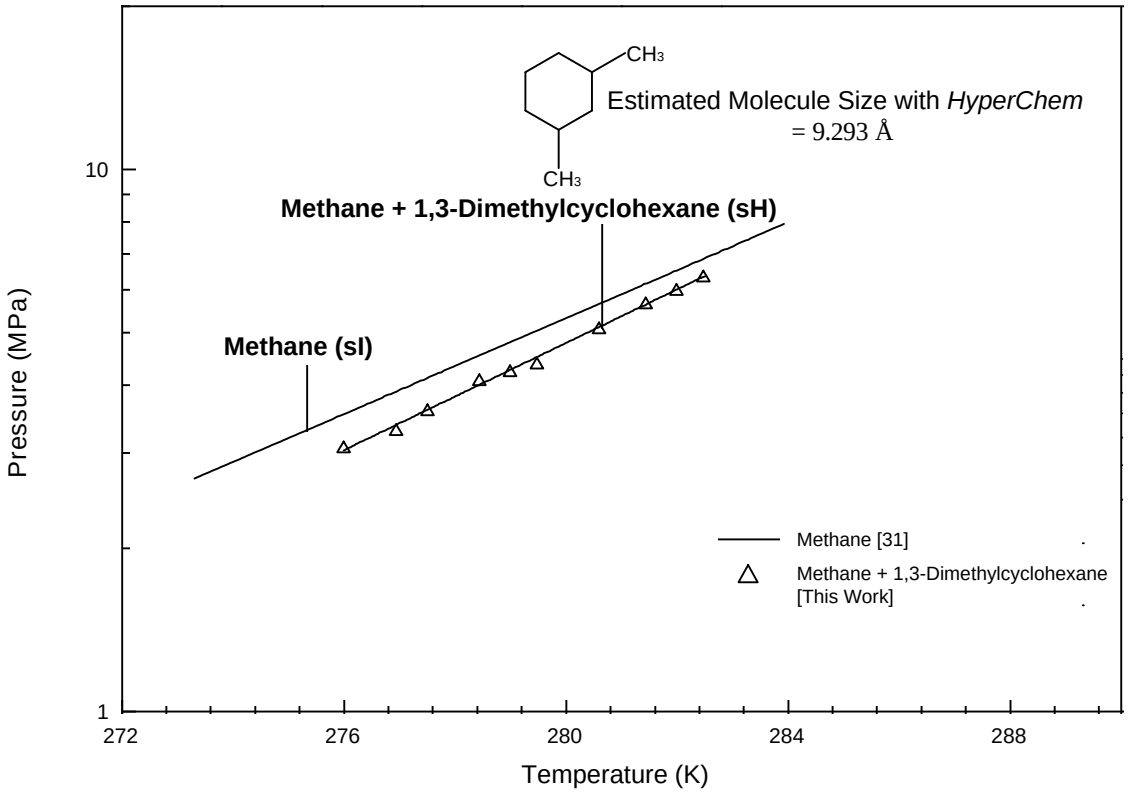

Figure 5: (Khokhar et al.)

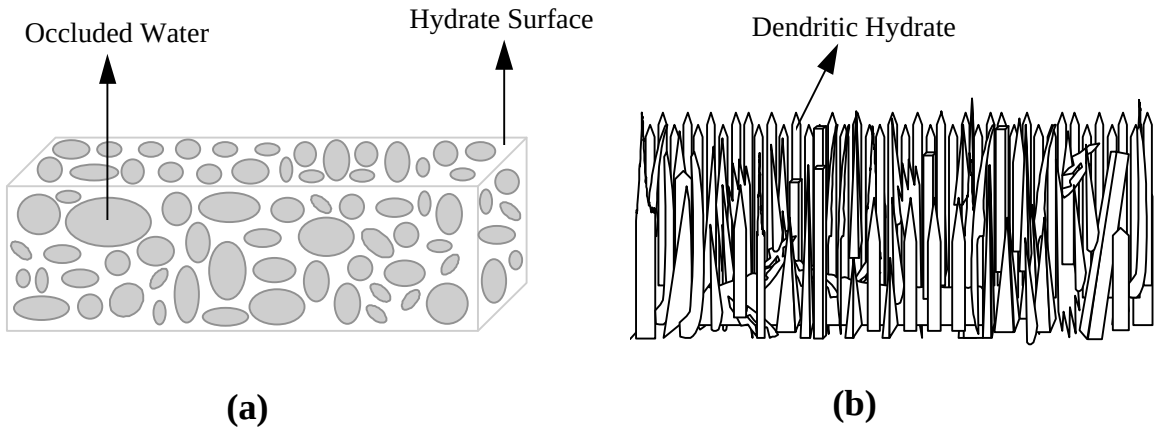

Figure 6: (Khokhar et al.)

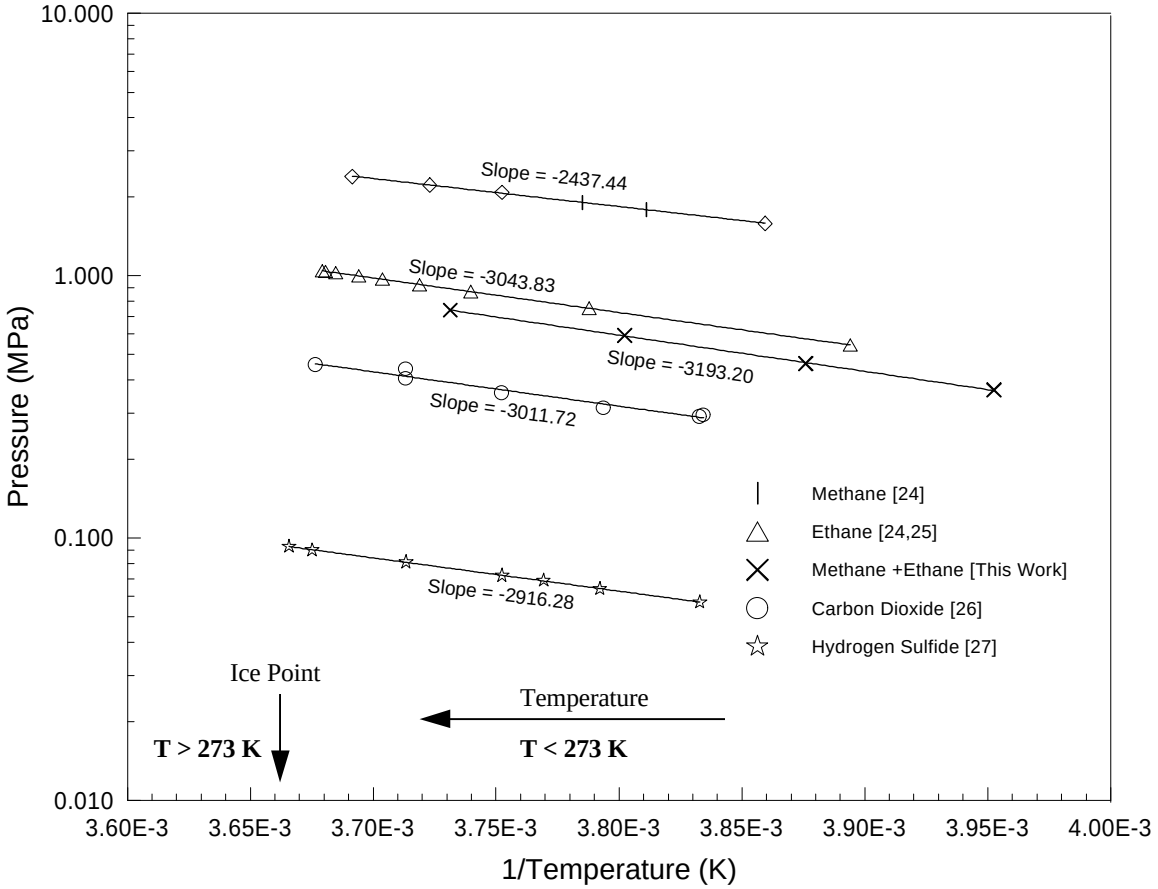

Figure 7: (Khokhar et al.)

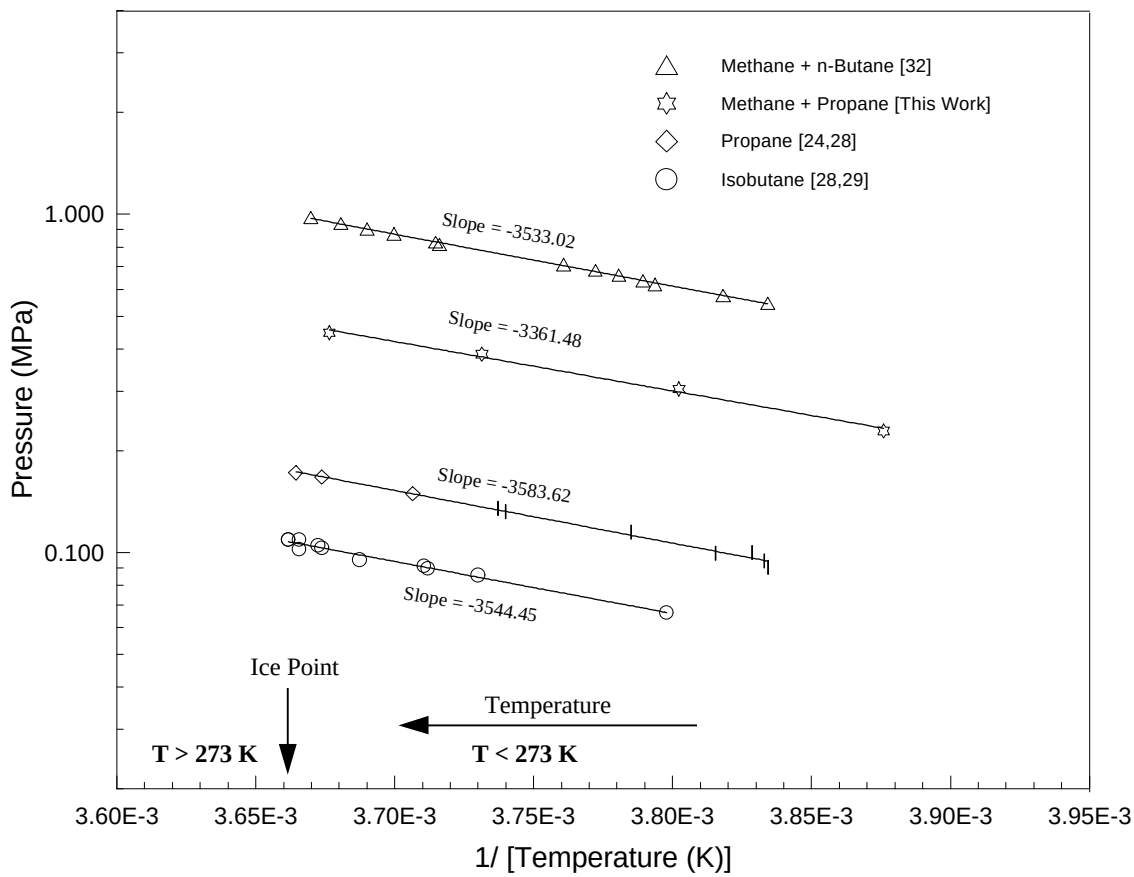

Figure 8: (Khokhar et al.)

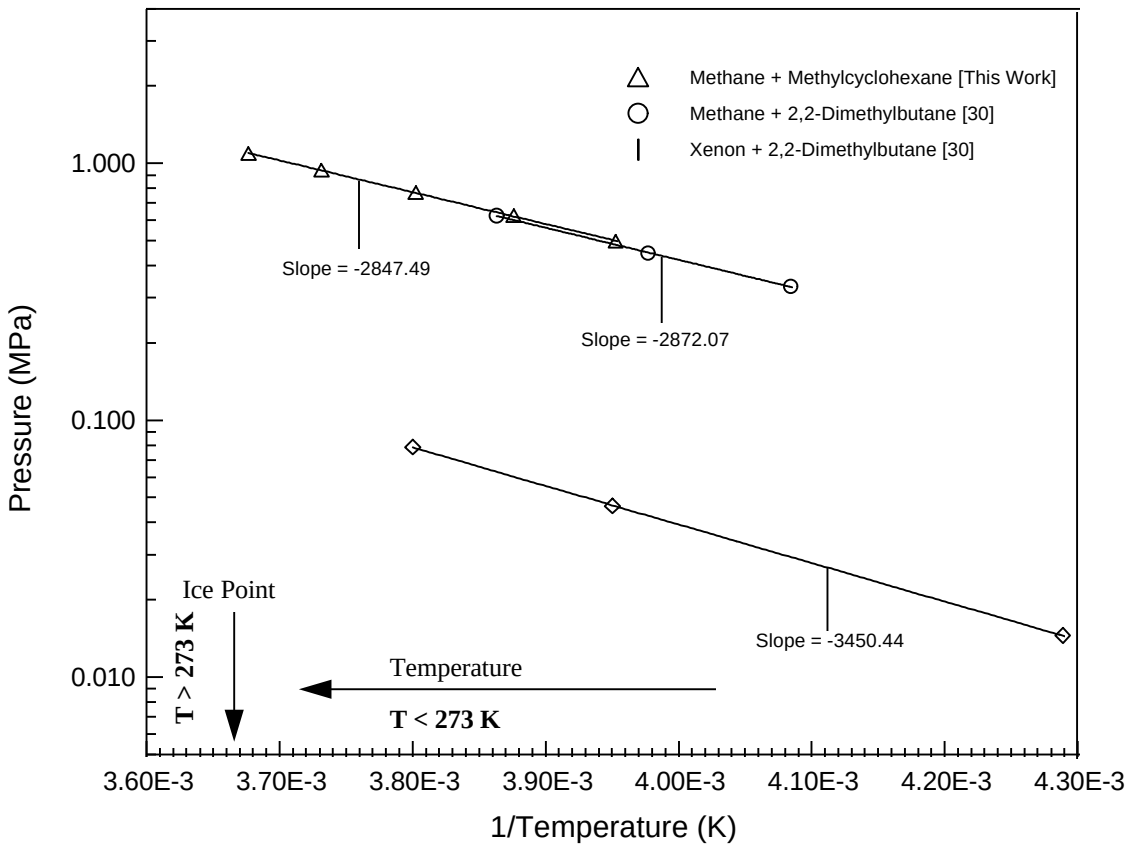

Figure 9: (Khokhar et al.)